

# Vibrational Circular Dichroism in Transition-Metal Complexes. 2. Ion Association, Ring Conformation, and Ring Currents of Ethylenediamine Ligands

Daryl A. Young, Teresa B. Freedman,\* Elmer D. Lipp, and Laurence A. Nafie\*

Contribution from the Department of Chemistry, Syracuse University, Syracuse, New York 13244. Received April 22, 1986

**Abstract:** Vibrational circular dichroism (VCD) has been used to probe the solution conformation of the ethylenediamine (en) ring in tris Co(III) and Cr(III) complexes. The VCD spectra in both the hydrogen stretching and mid-infrared regions are sensitive to the nature and concentration of the halide counterion. The halide anion can affect the ring conformation due to hydrogen bonding with the amino groups. The VCD results show that with excess chloride ion the  $\Lambda$  complex assumes the  $\delta\delta\delta$  conformation, and in aqueous solutions of  $\Lambda$ -[Co(en)<sub>3</sub>]<sup>3+</sup>, the mole fraction of rings in the  $\delta$  conformation is  $\sim 0.75$ . The biased VCD features in the NH and CH stretching and deformation regions of the complexes are interpreted in terms of vibrationally generated currents around the chelate ring or the ring formed by a bridging chloride ion. New empirical rules are presented for predicting the sense of ring current generated by the motion of adjacent methylene groups.

Recent advances in the interpretation of vibrational circular dichroism (VCD) spectra<sup>1,2</sup> have increased the utility of this technique as a probe of molecular conformation in solution. In particular, large, biased VCD has been attributed to vibrationally generated electronic currents in intramolecular rings.<sup>2-7</sup> The direction of the magnetic dipole transition moment is determined by the sense of the ring current resulting from a given phase of the driving nuclear oscillation. Rules governing the direction of ring current due to a bond contraction or elongation either external to or within a ring have been devised based on empirical results for a wide variety of molecules.<sup>2,5</sup> Coupled with a knowledge of the direction of the electric dipole transition moment, these rules lead to predictions of the sign of the VCD for the vibration, which depends both on the molecular conformation and configuration. Structural information can thus now be obtained from the VCD spectra without precise vibrational analysis or detailed intensity calculations. Both hydrogen-bonded and covalent rings have been found to provide pathways for ring current.

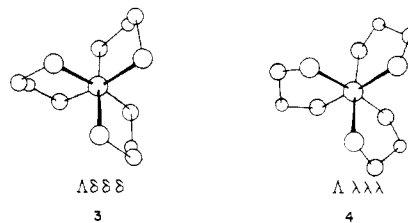
Two previous studies have involved rings closed by transition-metal coordination. In the CH stretching VCD of Cu(II) and Co(III) complexes of amino acids, the methine stretching VCD bias, due to current generated around the chelate ring, is increased in the complex compared to the free ligand.<sup>3b</sup> In a study of bis(acetylacetonato)(L-alaninato)cobalt(III), the greatly enhanced NH stretching VCD in the  $\Delta$  complex was attributed to current in a ring closed by a hydrogen bond between one N-H group and the lone pair on the adjacent acac oxygen.<sup>6</sup>

Chiral octahedral metal complexes have been a major focus of electronic circular dichroism studies, from which both configurational and conformational structures have been deduced.<sup>8</sup> The tris-chelated complexes of cobalt and chromium were among the first to be resolved into optical isomers and have formed the

basis for both theoretical and empirical studies.<sup>9</sup> The achiral ligand ethylenediamine (en) can assume the two enantiomeric puckered conformations **1** and **2** upon metal chelation



$\lambda$  and  $\delta$ , and in a tris complex these conformations are non-equivalent in energy due to interactions among the chelate rings. Corey and Bailar<sup>10</sup> determined that for the  $\Lambda$ -[Co(en)<sub>3</sub>]<sup>3+</sup> configuration, the  $\delta\delta\delta$  form, **3**, for which each C-C bond is nearly parallel to the C<sub>3</sub> axis of the complex (*lel* form) should be the most favored energetically, whereas the  $\lambda\lambda\lambda$  form, **4**, with the C-C



bonds oblique to the C<sub>3</sub> axis (*ob* form) is the least favored. A  $\delta \rightarrow \lambda$  inversion enthalpy of  $\sim 0.5$  kcal mol<sup>-1</sup> has been found.<sup>10,11</sup> However, the intermediate forms  $\lambda\delta\delta$  and  $\lambda\lambda\delta$  are statistically favored ( $RT \ln 3$ ) over the extreme forms by 0.7 kcal mol<sup>-1</sup>.<sup>12</sup> The form found by X-ray crystallography for [Co(en)<sub>3</sub>]<sup>3+</sup> or [Cr(en)<sub>3</sub>]<sup>3+</sup> salts depends on the anion present, presumably due to hydrogen-bonding interactions.<sup>13,14</sup> NMR studies<sup>11,15,16</sup> indicate that the aqueous solution conformation in the  $\Lambda$  complex is predominantly  $\delta$  ( $\sim 70\%$ ). The conformation was shown to be influenced by counterions, but the effect of halide ions was not investigated. The electronic CD spectra of a series of Co(III) complexes for which one or more rings are fixed in the *lel* ori-

(1) (a) Keiderling, T. A. *Appl. Spectrosc. Rev.* **1981**, *17*, 189. (b) Nafie, L. A. In *Vibrational Spectra and Structure*; Durig, J. R., Ed.; Elsevier: Amsterdam, 1981; Vol. 10, p 153. (c) Nafie, L. A. In *Advances in Infrared and Raman Spectroscopy*; Clark, R. J. M., Hester, R. E., Eds.; Wiley-Heyden: London, 1984; Vol. 11, p 49.

(2) Freedman, T. B.; Nafie, L. A. In *Topics in Stereochemistry*; Allinger, N. L., Eliel, E. L., Wilen, S. H., Eds.; Wiley: New York, 1987; Vol. 17, in press.

(3) (a) Nafie, L. A.; Oboodi, M. R.; Freedman, T. B. *J. Am. Chem. Soc.* **1983**, *105*, 7449. (b) Oboodi, M. R.; Lal, B. B.; Young, D. A.; Freedman, T. B.; Nafie, L. A. *J. Am. Chem. Soc.* **1985**, *107*, 1547.

(4) Paterlini, M. G.; Freedman, T. B.; Nafie, L. A. *J. Am. Chem. Soc.* **1986**, *108*, 1389.

(5) Freedman, T. B.; Balukjian, G. A.; Nafie, L. A. *J. Am. Chem. Soc.* **1985**, *107*, 6213.

(6) Young, D. A.; Lipp, E. D.; Nafie, L. A. *J. Am. Chem. Soc.* **1985**, *107*, 6205.

(7) Nafie, L. A.; Freedman, T. B. *J. Phys. Chem.* **1986**, *90*, 763.

(8) Mason, S. F. In *Optical Rotatory Dispersion and Circular Dichroism*; Ciardelli, F., Salvadori, P., Eds.; Heydon: London, 1973; pp 196-237.

(9) Kaufman, G. B. *Coord. Chem. Rev.* **1974**, *12*, 105.

(10) Corey, E. J.; Bailar, J. C., Jr. *J. Am. Chem. Soc.* **1959**, *81*, 2620.

(11) Hawkins, C. J.; Peachey, R. M. *Aust. J. Chem.* **1976**, *29*, 33.

(12) Piper, T. S.; Karipedes, A. G. *J. Am. Chem. Soc.* **1964**, *86*, 5039.

(13) Nakatsu, K.; Saito, Y.; Kuroya, H. *Bull. Chem. Soc. Jpn.* **1956**, *29*, 428.

(14) Raymond, K. N.; Corfield, P. W. R.; Ibers, J. A. *Inorg. Chem.* **1968**, *7*, 842.

(15) Sudmeier, J. L.; Blackmer, G. L.; Bradley, C. H.; Anet, F. A. L. *J. Am. Chem. Soc.* **1972**, *94*, 757.

(16) Hawkins, C. J.; Palmer, J. A. *Coord. Chem. Rev.* **1982**, *44*, 1.

entation reveal a sensitivity of the lowest energy d-electron transition to the ring conformation (as well as to the configuration) and suggest that a majority of the chelate rings in aqueous solutions of  $\Lambda$ -[Co(en)<sub>3</sub>]Cl<sub>3</sub> are  $\delta$ .<sup>8</sup> The effects of numerous anions, including halides, on the electronic CD have been reported, but no specific structures have been proposed for the interaction of [Co(en)<sub>3</sub>]<sup>3+</sup> with singly charged anions.<sup>17,18</sup>

Vibrational circular dichroism studies of tris-chelated Co(III) and Cr(III) complexes with achiral ligands provide an opportunity to investigate the ligand ring conformation in detail. The CD spectrum due to vibrational motions of the ligands provides a direct structural probe in contrast to the indirect effect of ring conformation on the electronic CD spectrum, and the presence of a paramagnetic nucleus such as Cr(III) does not interfere with VCD acquisition. These complexes are also of interest in furthering our understanding of the ring-current mechanism of VCD. We report here the results of VCD studies on the halide salts of tris(ethylenediamine)cobalt(III) and -chromium(III). Our studies focus on the dependence of ring conformation on solvent and counterion. We find that nearly all the VCD intensity in both the hydrogen stretching and mid-infrared regions can be attributed to vibrationally generated ring currents and that a quantitative determination of ring conformation can be obtained from the VCD spectra.

### Experimental Section

Both  $\Lambda$ - and  $\Delta$ -[Co(en)<sub>3</sub>]I<sub>3</sub>·H<sub>2</sub>O were prepared according to literature procedures.<sup>20</sup> The chloride or bromide salts were obtained by mixing the appropriate freshly precipitated silver halide with an aqueous solution of the iodide salt. The cobalt complexes were purified by recrystallization from aqueous solution by the addition of ethanol.

$\Lambda$ - and  $\Delta$ -[Cr(en)<sub>3</sub>]Cl<sub>3</sub>·H<sub>2</sub>O were prepared by resolution of the racemic complex.<sup>21,22</sup> The enantiomers were converted to the bromide or iodide salt by addition of NaBr or NaI to an aqueous solution of the chloride salt.<sup>23</sup> The chromium complexes were purified by recrystallization from aqueous solution by addition of methanol and were stored in the dark. Sample solutions were prepared immediately prior to use, and no decomposition was detected during the course of the VCD measurements.

The identity of each complex was confirmed by visible and infrared absorption and electronic circular dichroism spectroscopies.

The VCD and IR spectra for solutions prepared by using freshly opened Me<sub>2</sub>SO-*d*<sub>6</sub> (99.5% D, Stohler Isotope Chemicals) or D<sub>2</sub>O were obtained in a variable-path-length cell with CaF<sub>2</sub> windows. The spectra for solutions containing D<sub>2</sub>SO<sub>4</sub> or DCl were obtained with a demountable cell equipped with Infrasil windows and gasket, a 50- $\mu$ m spacer, and filling ports made of Teflon.

VCD spectra in the 3400–2800-cm<sup>-1</sup> region were recorded at 12-cm<sup>-1</sup> resolution on a dispersive VCD instrument constructed at Syracuse.<sup>24</sup> All the IR absorption and the mid-infrared VCD spectra were measured at 4-cm<sup>-1</sup> resolution with a modified Nicolet 7199 FTIR spectrometer as previously described.<sup>25</sup> In order to prevent detector saturation, a long-pass infrared filter (Optical Coatings Laboratory, Inc.) was used to remove light above 1600 cm<sup>-1</sup> in the FTIR–VCD measurements. Strong interference from Me<sub>2</sub>SO-*d*<sub>6</sub> solvent absorption precluded measurements below 1180 cm<sup>-1</sup>. VCD base lines were obtained from the average of the VCD spectra for both enantiomers.

### Results

The VCD and absorption spectra of Me<sub>2</sub>SO-*d*<sub>6</sub> solutions of the chloride, bromide, and iodide salts of  $\Lambda$ -[Co(en)<sub>3</sub>]<sup>3+</sup> are compared in Figure 1 for the NH and CH stretching regions and in Figure 2 for the mid-infrared region. The absorption and VCD fre-

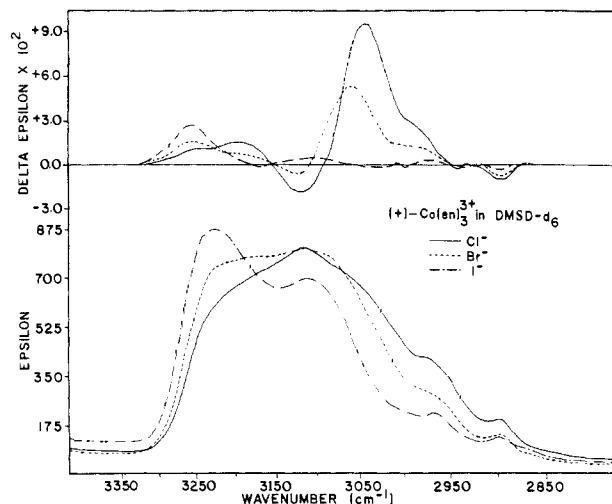


**Figure 1.** Absorption and VCD spectra of Me<sub>2</sub>SO-*d*<sub>6</sub> solutions of  $\Lambda$ -[Co(en)<sub>3</sub>]Cl<sub>3</sub> (—), 0.061 M,  $\Lambda$ -[Co(en)<sub>3</sub>]Br<sub>3</sub> (---), 0.063 M, and  $\Lambda$ -[Co(en)<sub>3</sub>]I<sub>3</sub> (· · ·) 0.067 M, in the hydrogen stretching region. The path length was 100  $\mu$ m.

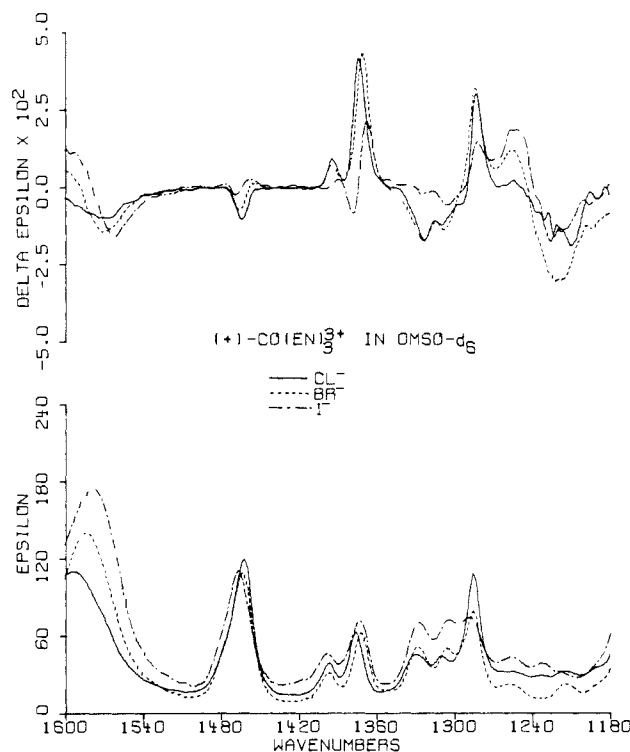


**Figure 2.** Mid-infrared absorption and VCD spectra of the chloride (—), bromide (---), and iodide (· · ·) salts of  $\Lambda$ -[Co(en)<sub>3</sub>]<sup>3+</sup> in Me<sub>2</sub>SO-*d*<sub>6</sub>, at concentrations of 0.072 M (Cl<sup>-</sup>), 0.085 M (Br<sup>-</sup>), and 0.063 M (I<sup>-</sup>) with a 380- $\mu$ m path length.

quencies and intensities are presented in Table I for [Co(en)<sub>3</sub>]I<sub>3</sub> and [Cr(en)<sub>3</sub>]I<sub>3</sub> in Me<sub>2</sub>SO-*d*<sub>6</sub>. The differences in frequency and intensity of the vibrational modes for the three salts clearly indicate a varying degree of interaction of the complex with the halide anion. Two absorption bands which can be ascribed to NH<sub>2</sub> antisymmetric and symmetric stretching modes (3225 and 3112 cm<sup>-1</sup>) are evident for the iodide salt. These features are broadened and shifted to a lower frequency and are no longer resolved in the spectra of the bromide and chloride salts. In the mid-infrared region, the NH<sub>2</sub> scissors absorption (~1580 cm<sup>-1</sup>) and the features below 1320 cm<sup>-1</sup> are quite sensitive to the anion, whereas the absorption features largely ascribed to methylene motion<sup>26,27</sup>

- (17) Smith, H. L.; Douglas, B. E. *Inorg. Chem.* **1966**, *5*, 784.  
 (18) Mason, S. F.; Norman, B. J. *J. Chem. Soc. A* **1966**, 307.  
 (19) Hawkins, C. J.; Peachey, R. M. *Acta Chem. Scand., Ser. A* **1978**, *32*, 815.  
 (20) Angelici, R. J. In *Synthesis and Technique in Inorganic Chemistry*; Saunders: Philadelphia, 1977; pp 71–80.  
 (21) Pederson, E. *Acta Chem. Scand.* **1970**, *24*, 3362.  
 (22) Galsbol, F. *Inorg. Synth.* **1970**, *12*, 240.  
 (23) Rollinson, C.; Bailar, J. C., Jr. *Inorg. Synth.* **1946**, *2*, 196.  
 (24) (a) Diem, M.; Gotkin, P. J.; Kupfer, J. M.; Nafie, L. A. *J. Am. Chem. Soc.* **1978**, *100*, 5644. (b) Diem, M.; Photos, E.; Khouri, H.; Nafie, L. A. *J. Am. Chem. Soc.* **1979**, *101*, 6829. (c) Lal, B. B.; Diem, M.; Polavarapu, P. L.; Oboodi, M.; Freedman, T. B.; Nafie, L. A. *J. Am. Chem. Soc.* **1982**, *104*, 3336. (d) Oboodi, M. R. Ph.D. Thesis, Syracuse University, 1982.  
 (25) Lipp, E. D.; Nafie, L. A. *Appl. Spectrosc.* **1984**, *38*, 20.

- (26) Gouteron, J. *J. Inorg. Nucl. Chem.* **1976**, *38*, 63.  
 (27) James, D. W.; Nolan, M. J. *Inorg. Nucl. Chem. Lett.* **1973**, *9*, 319.

**Table I.** Frequencies, Intensities, and Assignments of the Absorption and VCD Bands of  $\Lambda$ -[M(en)<sub>3</sub>]I<sub>3</sub> in Me<sub>2</sub>SO-d<sub>6</sub>

$\Lambda$ -[Co(en) <sub>3</sub> ]I <sub>3</sub>				$\Lambda$ -[Cr(en) <sub>3</sub> ]I <sub>3</sub>				assign <sup>a</sup>
absorption		VCD		absorption		VCD		
freq, cm <sup>-1</sup>	$\epsilon$ , 10 <sup>3</sup> cm <sup>2</sup> /mol <sup>-1</sup>	freq, cm <sup>-1</sup>	10 <sup>3</sup> $\Delta\epsilon$ , 10 <sup>3</sup> cm <sup>2</sup> mol <sup>-1</sup>	freq, cm <sup>-1</sup>	$\epsilon$ , 10 <sup>3</sup> cm <sup>2</sup> mol <sup>-1</sup>	freq, cm <sup>-1</sup>	10 <sup>3</sup> $\Delta\epsilon$ , 10 <sup>3</sup> cm <sup>2</sup> mol <sup>-1</sup>	
3225	775	3225	+27	3210	773	3250	+14	$\nu^a$ (NH <sub>2</sub> )
		3192	+4.5					
3112	605	3112	+4.5	3085	632	3050	-8.0	$\nu^s$ (NH <sub>2</sub> )
		3030	-1.8					
2965	80	2975	+2.0	2968	118	2968	+2.0	$\nu^a$ (CH <sub>2</sub> )
2900	64	2893	-2.0	2900	85	2890	-2.0	$\nu^s$ (CH <sub>2</sub> )
1578	153	1562	-15	1568	185	1552	-40	$\delta$ (NH <sub>2</sub> )
1466	89	1469	-2.0	1467	95	1473	-2.0	$\delta$ (CH <sub>2</sub> )
		1456	+2.0			1461	+5.0	
1398	24	1389	+3.0	1398	15	1390	+3.0	$\omega$ (CH <sub>2</sub> )
1373	49	1371	-8.0	1372	31	1376	-5.0	
		1367	+22			1368	+13	
1327	46	1325	-2.0	1333	61	1329	+3.0	$\tau$ (CH <sub>2</sub> )
1304	46	1305	-5.0	1303	119	1300	-8.0	$\omega$ (CH <sub>2</sub> )
1288	47	1283	+16	1282	67	1282	+12	$\tau$ (NH <sub>2</sub> )
1255	16	1253	+20					
1231	12			1231	18	1228	+21	
1218	5	1216	-16	1209	26	1203	-18	$\nu^a$ (C-N)
1191	7							

<sup>a</sup>  $\nu^a$  = antisymmetric stretch,  $\nu^s$  = symmetric stretch,  $\delta$  = scissors,  $\omega$  = wag, and  $\tau$  = twist.

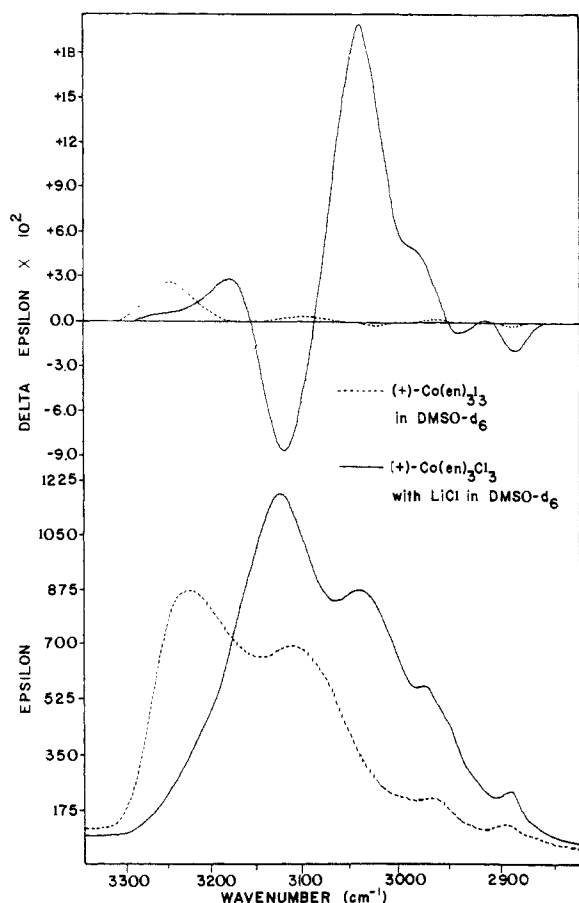


**Figure 3.** Comparison of the hydrogen stretching absorption and VCD spectra of  $\Lambda$ -[Co(en)<sub>3</sub>]I<sub>3</sub> (---), 0.067 M, and  $\Lambda$ -[Co(en)<sub>3</sub>]Cl<sub>3</sub> (—), 0.060 M with 0.6 M LiCl, in Me<sub>2</sub>SO-d<sub>6</sub> at a 100- $\mu$ m path length.

(~1460, 1395, and 1375 cm<sup>-1</sup>) exhibit smaller variations. The VCD spectra exhibit large variations for both the NH<sub>2</sub> and CH<sub>2</sub> motions when the anion is changed from iodide to either chloride or bromide.

Compared to the Co(III) complexes, the spectra in the methylene regions for the corresponding Cr(III) complexes<sup>28</sup> are nearly identical in form and frequency but are somewhat weaker in VCD

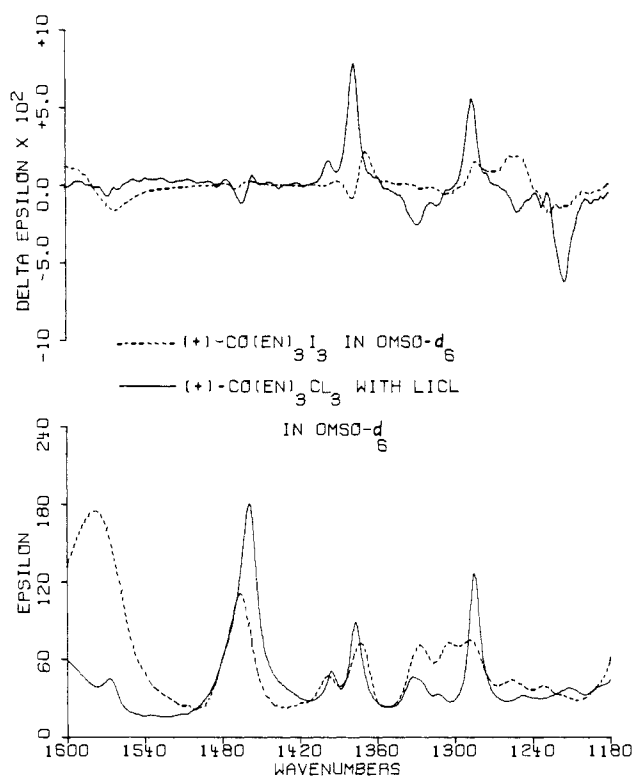


**Figure 4.** Effects of excess chloride ion on the mid-infrared absorption and VCD spectra of  $\Lambda$ -[Co(en)<sub>3</sub>]<sup>3+</sup> in Me<sub>2</sub>SO-d<sub>6</sub>: (---) iodide salt, 0.063 M, and (—) chloride salt, 0.06 M plus 0.6 M LiCl. Path length was 380  $\mu$ m.

intensity. The NH<sub>2</sub> scissors mode exhibits increased absorption and VCD intensity and decreased frequency in the Cr(III) complex. Distinct variations in frequency and intensity upon changing from Co(III) to Cr(III) are also observed for the modes below 1350 cm<sup>-1</sup>, which is suggestive of participation of nitrogen or amino motion in these vibrational modes. It is also of interest to note that for both metals the mid-infrared modes ascribed largely to CH<sub>2</sub> motion increase in absorption intensity when the anion is changed from iodide to chloride.

The spectral variations in Figures 1 and 2 are consistent with a hydrogen-bonding interaction between the chloride or bromide anions and some but not all of the NH<sub>2</sub> groups in the complex. The appearance of only two well-resolved absorption features in

(28) Young, D. A. Ph.D. Thesis, Syracuse University, 1986.

**Table II.** Frequencies, Intensities, and Assignments of the Absorption and VCD Spectra of  $\Lambda$ -[Co(en)<sub>3</sub>]Cl<sub>3</sub> in 0.6 M LiCl/Me<sub>2</sub>SO-*d*<sub>6</sub> Solution

absorption		VCD		assign <sup>a</sup>
freq, cm <sup>-1</sup>	$\epsilon$ , 10 <sup>3</sup> cm <sup>2</sup> mol <sup>-1</sup>	freq, cm <sup>-1</sup>	10 <sup>3</sup> $\Delta\epsilon$ , 10 <sup>3</sup> cm <sup>2</sup> mol <sup>-1</sup>	
		3225	+6.7	
		3180	+28	
3125	1098	1229	-89	$\nu^s(\text{NH}_2)$
3041	792	3041	+200	$\nu^s(\text{NH}_2)$
2975	(52) <sup>b</sup>	2975	+43	$\nu^s(\text{CH}_2)$
2952	(105) <sup>b</sup>	2945	-8.3	2 × $\delta(\text{CH}_2)$
2893	(118) <sup>b</sup>	2890	-23	$\nu^s(\text{CH}_2)$
1568	31	1596	-6.0	
1459	160	1466	-14	$\delta(\text{CH}_2)$
1396	29	1397	+15	$\omega(\text{CH}_2)$
1377	65	1377	+78	
1331	22	1327	-25	$\tau(\text{CH}_2)$
1314	6	1313	-13	$\omega(\text{NH}_2)$
1285	98	1286	+55	$\tau(\text{NH}_2)$
1248	3			
1212	6	1215	-62	$\nu^s(\text{C-N})$

<sup>a</sup>See Table I. <sup>b</sup>Methylene stretching absorption intensities were obtained from spectrum of racemic Co(D<sub>2</sub>NCH<sub>2</sub>CH<sub>2</sub>ND<sub>2</sub>)<sub>3</sub>Cl<sub>3</sub> in 0.6 M LiCl/Me<sub>2</sub>SO-*d*<sub>6</sub>.

the NH<sub>2</sub> stretching region of [Co(en)<sub>3</sub>]I<sub>3</sub> indicates that this type of interaction is weak or absent when only iodide is present. The sensitivity of the methylene VCD spectra to the nature of the anion suggests alterations in ring conformation due to the hydrogen bonding in the chloride and bromide salts. Further support for this interpretation is provided in Figures 3 and 4 and Table II, in which the VCD and absorption spectra of the iodide salt of  $\Lambda$ -[Co(en)<sub>3</sub>]<sup>3+</sup> in Me<sub>2</sub>SO-*d*<sub>6</sub> are compared with those of a Me<sub>2</sub>SO-*d*<sub>6</sub> solution of the chloride salt saturated with LiCl, a 10-fold excess of chloride anion per complex. The NH<sub>2</sub> stretching modes (Figure 3) occur as two distinct absorption bands in both solutions but exhibit a shift to lower frequency and an increase in intensity with excess chloride ion present. This behavior is consistent with an equivalent hydrogen-bonding interaction in the latter solution between each NH<sub>2</sub> group of the complex and chloride ion. In the mid-infrared region (Figure 4) the NH<sub>2</sub> scissors mode shifts to above 1600 cm<sup>-1</sup> and apparently decreases in intensity, also indicative of NH<sub>2</sub>...Cl interaction. The absorption spectrum of this band could not be observed due to solvent interference. The modes at 1459, 1396, 1377, and 1285 cm<sup>-1</sup> exhibit increased absorption intensity with excess chloride ion compared to the chloride salt in Figure 2.

The alteration in the VCD spectrum of the complex upon addition of excess chloride ion is dramatic. The NH<sub>2</sub> stretching modes (Figure 3) give rise to two very intense VCD bands of opposite sign located at the absorption maxima. The bisignate VCD character noted for some mid-infrared modes in the iodide salt is absent. At high chloride concentration the VCD corresponding to each absorption band in Figures 3 and 4 is observed as a single monosignate feature. The maximum of the NH<sub>2</sub> scissors absorption was not observed due to the 1600-cm<sup>-1</sup> cutoff of the experiment, but practically no VCD signal is observed at 1600 cm<sup>-1</sup>, which is within the absorption band. The weak absorption feature at 1212 cm<sup>-1</sup> gives rise to a VCD band with an anisotropy ratio of -0.01, one of the largest values thus far recorded.

In order to specify the mid-infrared assignments further, the hydrogens on the amino groups of the racemic chloride complex were exchanged in D<sub>2</sub>O, and the IR absorption spectrum of [Co(en)<sub>3</sub>]Cl<sub>3</sub>-*N-d*<sub>12</sub> was recorded in Me<sub>2</sub>SO-*d*<sub>6</sub> saturated with LiCl. Bands at 1460, 1395, 1374, 1344, and 1266 cm<sup>-1</sup> are observed for the deuterated complex, which correlate with the bands at 1459, 1396, 1377, 1332, and 1275 cm<sup>-1</sup> in the parent complex. The ND<sub>2</sub> scissors mode is observed as a strong band at 1220 cm<sup>-1</sup> which obscures any weak features which may correspond to the 1248- and 1212-cm<sup>-1</sup> band in the spectrum of the -*N*-H<sub>12</sub> complex. These results indicate that the features at

**Table III.** Frequencies, Intensities, and Assignments of the Absorption and VCD Spectra of  $\Lambda$ -[M(en)<sub>3</sub>]<sup>3+</sup> Salts in Acidic Aqueous Solution

absorption		VCD		assign <sup>a</sup>
freq, cm <sup>-1</sup>	$\epsilon$ , 10 <sup>3</sup> cm <sup>2</sup> mol <sup>-1</sup>	freq, cm <sup>-1</sup>	10 <sup>3</sup> $\Delta\epsilon$ , 10 <sup>3</sup> cm <sup>2</sup> mol <sup>-1</sup>	
$\Lambda$ -[Co(en) <sub>3</sub> ]I <sub>3</sub> in 1 M D <sub>2</sub> SO <sub>4</sub>				
3250	700	3280	+19	$\nu^s(\text{NH}_2)$
		3215	+4.0	
3138	595	3122	-6.0	$\nu^s(\text{NH}_2)$
		3075	-3.0	
2978	46	2984	+2.6	$\nu^s(\text{CH}_2)$
2908	34	2899	-2.0	$\nu^s(\text{CH}_2)$
$\Lambda$ -[Cr(en) <sub>3</sub> ]Cl <sub>3</sub> in 1 M D <sub>2</sub> SO <sub>4</sub>				
3240	685	3275	+16	$\nu^s(\text{NH}_2)$
		3215	+3.0	
3130	510	3115	-4.5	$\nu^s(\text{NH}_2)$
		3080	-5.0	
2982	53	2979	+1.6	$\nu^s(\text{CH}_2)$
2906	38	2899	-1.7	$\nu^s(\text{CH}_2)$
$\Lambda$ -[Co(en) <sub>3</sub> ]I <sub>3</sub> in 1 M DCl				
3240	566	3275	+18	$\nu^s(\text{NH}_2)$
		3210	+6.0	
3129	491	3115	+3.3	$\nu^s(\text{NH}_2)$
		3068	-1.0	
2982	51	2982	+2.2	$\nu^s(\text{CH}_2)$
2908	34	2899	-1.9	$\nu^s(\text{CH}_2)$
$\Lambda$ -[Co(en) <sub>3</sub> ]Cl <sub>3</sub> in 1 M DCl				
3242	561	3276	+16	$\nu^s(\text{NH}_2)$
		3215	+4.0	
		3165	-1.3	
3130	486	3105	+2.5	$\nu^s(\text{NH}_2)$
		3060	-1.5	
2982	51	2982	+2.0	$\nu^s(\text{CH}_2)$
2908	54	2899	-1.7	$\nu^s(\text{CH}_2)$
$\Lambda$ -[Co(en) <sub>3</sub> ]Cl <sub>3</sub> in 1 M DCl				
3205	706	3265	+11	$\nu^s(\text{NH}_2)$
3118	577	3118	+28	$\nu^s(\text{NH}_2)$
2982	46	2982	+6.5	$\nu^s(\text{CH}_2)$
2906	34	2899	-5.8	$\nu^s(\text{CH}_2)$

<sup>a</sup>See Table I.

1459 cm<sup>-1</sup>, assigned to the CH<sub>2</sub> scissors, and those at 1396 and 1377 cm<sup>-1</sup>, assigned to the CH<sub>2</sub> wag, are localized methylene modes, whereas below 1350 cm<sup>-1</sup> the normal modes consist of contributions from CH<sub>2</sub>, NH<sub>2</sub>, C-N, and C-C motions and are thus more dispersed over the entire ligand.

In D<sub>2</sub>O solution, exchange of the amine protons with deuterium can be prevented by the addition of acid, thus permitting the observation of the NH<sub>2</sub> stretching VCD in aqueous solution, shown in Figure 5 and Table III. In 1 M D<sub>2</sub>SO<sub>4</sub>, or 1 and 6 M DCl solutions, distinct absorption and VCD features are observed for the antisymmetric and symmetric NH<sub>2</sub> stretches and CH<sub>2</sub> stretches for either the chloride or the iodide salts. The strength of the hydrogen bonding to the halide is apparently significantly reduced in D<sub>2</sub>O compared to that in Me<sub>2</sub>SO-*d*<sub>6</sub>, since the latter has a lower dielectric constant and is aprotic. In D<sub>2</sub>SO<sub>4</sub>, the weak VCD observed in each of the two NH<sub>2</sub> stretching regions is opposite in sign to that observed with excess chloride in Me<sub>2</sub>SO-*d*<sub>6</sub>. In 1 M DCl, the symmetric NH<sub>2</sub> stretching VCD becomes positive. In 6 M DCl, the NH<sub>2</sub> modes are shifted ~10 cm<sup>-1</sup> to lower frequency and exhibit an increase in intensity compared to the iodide salt in D<sub>2</sub>SO<sub>4</sub>, and the symmetric NH<sub>2</sub> stretching VCD intensity becomes considerably more positive with little corresponding change in the antisymmetric mode, as compared to 1 M DCl. The antisymmetric NH<sub>2</sub> stretching VCD intensity in acidic D<sub>2</sub>O is the same sign but slightly weaker than that for the iodide salt in Me<sub>2</sub>SO-*d*<sub>6</sub>.

The methylene stretching modes observed in acidic D<sub>2</sub>O are considerably weaker than the NH<sub>2</sub> stretches. In neutral D<sub>2</sub>O solution deuterium exchange removes interference from the amine

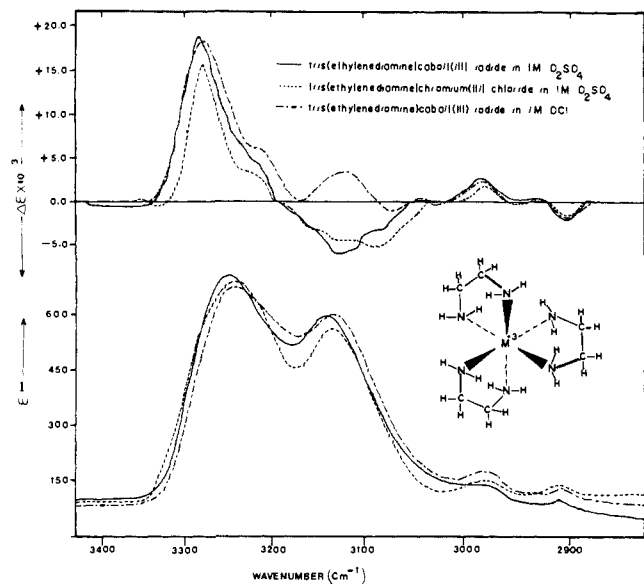


**Figure 5.** NH and CH stretching absorption and VCD spectra of ethylenediamine complexes in acidic solution: (—)  $\Delta$ -[Co(en)<sub>3</sub>]I<sub>3</sub>, 0.07 M in 1 M DCl; (---)  $\Delta$ -[Cr(en)<sub>3</sub>]Cl<sub>3</sub>, 0.11 M in 1 M D<sub>2</sub>SO<sub>4</sub>; and (-·-)  $\Delta$ -[Co(en)<sub>3</sub>]I<sub>3</sub>, 0.10 M in 1 M DCl. Path length was 50  $\mu$ m.

**Table IV.** Frequencies, Intensities, and Assignments of the Absorption and VCD Spectra of Methylene Stretching Modes in [Co(en)<sub>3</sub>]<sup>3+</sup> Salts

absorption		VCD		assign <sup>a</sup>
freq, cm <sup>-1</sup>	$\epsilon$ , 10 <sup>3</sup> cm <sup>2</sup> mol <sup>-1</sup>	freq, cm <sup>-1</sup>	10 <sup>3</sup> Δ $\epsilon$ , 10 <sup>3</sup> cm <sup>2</sup> mol <sup>-1</sup>	
$\Delta$ -[Co(en) <sub>3</sub> ]I <sub>3</sub> /D <sub>2</sub> O				
2976	30	2989	+1.3	$\nu^{\delta}(\text{CH}_2)$
2949	9			2 × $\delta(\text{CH}_2)$
2910	30	2908	-1.0	$\nu^{\delta}(\text{CH}_2)$
$\Delta$ -[Co(en) <sub>3</sub> ]Cl <sub>3</sub> /D <sub>2</sub> O				
2976	29	2990	+2.2	$\nu^{\delta}(\text{CH}_2)$
2949	10			2 × $\delta(\text{CH}_2)$
2940	9			
2910	28	2905	-1.3	$\nu^{\delta}(\text{CH}_2)$
$\Delta$ -[Co(en) <sub>3</sub> ]Cl <sub>3</sub> in 2 M NaCl/D <sub>2</sub> O				
2976	30	2992	+2.9	$\nu^{\delta}(\text{CH}_2)$
2949	11			2 × $\delta(\text{CH}_2)$
2941	11			
2912	31	2907	-1.9	$\nu^{\delta}(\text{CH}_2)$

<sup>a</sup>See Table I.

stretches, allowing longer path lengths to be employed, Figure 6 and Table IV. Although increases in the CH<sub>2</sub> stretching VCD intensity are observed with excess chloride ion in aqueous solution, these changes are not nearly as dramatic as the 10-fold increase observed in [Co(en)<sub>3</sub>]Cl<sub>3</sub> with excess chloride compared to [Co(en)<sub>3</sub>]I<sub>3</sub> in Me<sub>2</sub>SO-*d*<sub>6</sub>. The absorption spectra of Me<sub>2</sub>SO-*d*<sub>6</sub> solutions of the complexes with deuterated amino groups reveal that the presence of excess chloride causes a large increase in the symmetric CH<sub>2</sub> stretching intensity and a strong increase in Fermi resonance with the overtone of the CH<sub>2</sub> scissors, due to a shift in the scissors frequency from 1467 cm<sup>-1</sup> in the iodide to 1460 cm<sup>-1</sup> in excess chloride and an increase in the scissors intensity.

## Discussion

**Ethylenediamine Ring Conformation.** The occurrence of two well-defined NH<sub>2</sub> stretching absorption features in the IR spectrum of  $\Delta$ -[Co(en)<sub>3</sub>]Cl<sub>3</sub> in Me<sub>2</sub>SO-*d*<sub>6</sub> with excess chloride (Figure 3), which have shifted to a lower frequency and have increased in intensity compared to the corresponding bands for the iodide salt, is indicative of a structure with all six NH<sub>2</sub> groups involved in an equivalent hydrogen-bonding interaction with chloride ion. Furthermore, the large enhancement of the methylene VCD intensities and the monosignate character of these VCD bands with

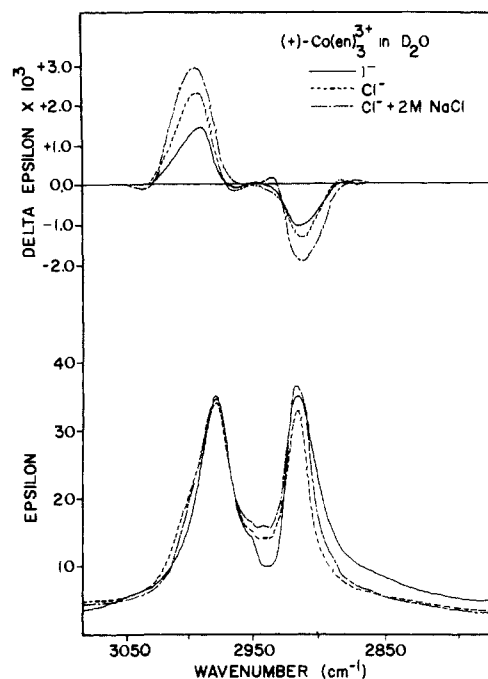


**Figure 6.** Absorption and VCD spectra in the CH-stretching region of  $\Delta$ -[Co(en)<sub>3</sub>]<sup>3+</sup>, 0.10 M in D<sub>2</sub>O, 200  $\mu$ m path length: (—) iodide salt, (---) chloride salt, (-·-) chloride salt plus 2 M NaCl.

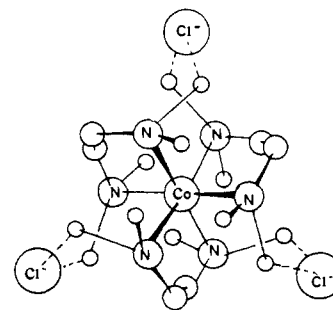


**Figure 7.** Structure of  $\Delta$ -[Co(en)<sub>3</sub>]<sup>3+</sup> cation with three chloride ions bridging pairs of amino groups, viewed along the C<sub>3</sub> axis. Complex has D<sub>3</sub> symmetry and all en rings are in the  $\delta$  conformation.

excess chloride present implies that all the rings possess the same conformation, the more favorable  $\delta$  form for the  $\Delta$  configuration. In crystalline  $\Delta$ -[Co(en)<sub>3</sub>]Cl<sub>3</sub>·H<sub>2</sub>O two of the chloride counterions lie along pseudo-C<sub>2</sub> axes of the complex, forming hydrogen-bonded bridges between two pairs of amino groups.<sup>29</sup> The structure proposed for  $\Delta$ -[Co(en)<sub>3</sub>]<sup>3+</sup> in solution containing excess chloride ion, shown in Figure 7, has three such bridging chloride ions. This complex has D<sub>3</sub> symmetry since the chloride bridges force the complex to assume the  $\Delta$ - $\delta\delta\delta$  structure.

At lower chloride or bromide concentrations in Me<sub>2</sub>SO-*d*<sub>6</sub>, the NH<sub>2</sub> stretching absorption spectra are indicative of a mixture of hydrogen-bonded and free amino groups, and in the iodide salt, little interaction with the anion is evident. The concurrent decrease in methylene VCD intensity and the appearance of some bisignate character in the mid-infrared methylene VCD bands is characteristic of samples with a mixture of  $\lambda$  and  $\delta$  ring conformations. In neutral and acidic aqueous solutions the spectral effects of chloride binding are still evident, although not as dramatic as in Me<sub>2</sub>SO.

The changes in the VCD spectra of [Co(en)<sub>3</sub>]<sup>3+</sup> due to changes in the solvent or in the nature and concentration of the counterion can arise both from variations in the relative amounts of  $\delta$  and  $\lambda$  ring conformations and from changes in the mechanism by which the VCD signal is generated, as will be discussed below. Therefore,

(29) Iwata, M.; Nakatsu, K.; Saito, Y. *Acta Crystallogr., Sect. B: Struct. Sci.* 1969, 25, 2562.

the VCD intensities need not always be linearly related to the abundance of a particular ring conformation. Consistent evidence from other types of investigations<sup>8</sup> indicate that in aqueous solution, the  $\Delta$  configuration will have an excess of the  $\delta$  ring conformation 2. The CH stretching VCD spectra for the deuterated complex in  $D_2O$ , Figure 6, consists of monosignate features in the anti-symmetric and symmetric methylene stretching regions which vary in intensity with chloride concentration but maintain the same sign. These features are due to very localized motion with little contribution from other coordinates, since the amino groups are deuterated. The bands shift only slightly in position with chloride concentration, indicative of nearly equal  $CH_2$  stretching frequencies for the  $\delta$  and  $\lambda$  conformations, and the absorption intensities remain nearly constant. It is reasonable, therefore, that a single ethylenediamine ring in the  $\delta$  conformation contributes VCD intensity which is equal in magnitude, but opposite in sign, to that of a single ring in the  $\lambda$  configuration and that the magnitude of this contribution is not influenced by the presence or concentration of chloride ion, which forces the complex into the  $\delta$  form. The CH stretching VCD intensity in the  $D_2O$  solutions therefore does reflect the excess of the  $\delta$  over the  $\lambda$  conformation. Similarly, in acidic aqueous solution, the methylene absorption intensities and frequencies remain constant, and these bands are well resolved from the  $NH_2$  stretching modes.

If the VCD spectrum of the 100%  $\delta\delta\delta$  form can be obtained, for example at high chloride concentration, the mole fraction,  $n_\delta$ , of the  $\delta$  conformation at lower anion concentrations can be derived from the ratio of the integrated areas of the VCD bands through the relationship  $n_\delta = (\Delta\epsilon/\Delta\epsilon_{100\%} + 1)/2$ . In the electronic CD spectra,<sup>17</sup> the maximum increase in the rotational strength due to the addition of chloride is reached at 2 M  $Cl^-$ . With the VCD intensity for  $[Co(en)_3]^{3+}$  in aqueous 2 M NaCl solution taken as  $\Delta\epsilon_{100\%}$ , we find the upper limits of  $n_\delta \leq 0.75 \pm 0.03$  for the iodide salt and  $n_\delta \leq 0.84 \pm 0.03$  for the chloride salt as an average over the two  $CH_2$  stretching bands. In acidic solution, with the intensities in 6 M DCl as  $\Delta\epsilon_{100\%}$ ,  $n_\delta = 0.67 \pm 0.001$  for  $\Delta-[Co(en)_3]^{3+}$  in either 1 M DCl or 1 M  $D_2SO_4$ . The mole fraction  $n_\delta$  for the chromium complex in 1 M  $D_2SO_4$  is  $0.64 \pm 0.01$ . These values of  $n_\delta$  can be compared with values obtained by NMR vicinal coupling constants,  $0.70 \pm 0.07$  for  $\Delta-[Co(en)_3]^{3+}$  in  $D_2O$  (counterion not specified) and  $0.83 \pm 0.08$  for the complex in 0.3 M phosphate.<sup>11</sup> With the NMR chemical shift method,  $n_\delta$  for  $\Delta-[Ni(en)_3]^{2+}$  in water was determined to be 0.60 (nitrate counterion), 0.62 (chloride counterion), and 0.65 in 1.6 M NaCl.<sup>19</sup>

In contrast to the minor influence of chloride ion on the  $CH_2$  stretching absorption intensities in water, addition of chloride in  $Me_2SO-d_6$  causes a large increase in the intensity of the symmetric  $CH_2$  stretch and a large increase in the Fermi resonance between the symmetric  $CH_2$  stretch and the scissors overtone. Thus there appears to be a stronger direct interaction between the chloride ion and the methylene hydrogens in  $Me_2SO-d_6$  as compared to  $D_2O$ . In addition, there may be some contribution from  $NH_2$  stretching motion in the  $CH_2$  stretching modes in  $Me_2SO$  at high chloride concentration.

For these reasons, the CH stretching modes in  $Me_2SO$  are no longer reliable probes for the quantitative measurement of ring conformation. Similar difficulties may arise from the mid-infrared modes. However, qualitatively, it is clear that iodide ion has the weakest interaction with both the Cr(III) and Co(III) complexes, and the interaction of bromide is similar to but slightly weaker than that of chloride. The NH stretching VCD spectra show that the strength of the interaction with anion is clearly diminished in acidic aqueous solution compared to that in  $Me_2SO-d_6$ .

**Ring-Current Mechanism.** VCD intensity is proportional to the rotational strength,  $R = \text{Im}(\mu \cdot m)$ , where  $\mu$  is the electric dipole transition moment,  $m$  is the magnetic dipole transition moment, and  $\text{Im}$  denotes the imaginary part. For a fundamental transition of normal mode  $Q_a$  having conjugate momentum  $P_a$ , it can be shown that<sup>7</sup>

$$R = \frac{\hbar}{2} \left( \frac{\partial \mu}{\partial Q_a} \right)_{0,0} \left( \frac{\partial m}{\partial P_a} \right)_{0,0}$$

where 0,0 denotes equilibrium values of both nuclear position and momentum. Thus, for non-zero VCD, during the vibration there must be simultaneously a linear oscillation of charge  $(\partial \mu / \partial Q_a)_0$  and an angular or circular oscillation of charge  $(\partial m / \partial P_a)_0$ .

The vibrational modes of  $[Co(en)_3]^{3+}$  above  $1300 \text{ cm}^{-1}$  arise primarily from motions localized at the methylene or amino groups.<sup>26,27</sup> For each ring the two local  $NH_2$  or  $CH_2$  motions can couple to form modes which are symmetric (A) or antisymmetric (B) with respect to the  $C_2$  axis of the ring. Below  $\sim 1300 \text{ cm}^{-1}$ , the C-C and C-N ring stretches mix with the A or B methylene and amino rocking and twisting motions to give rise to normal modes more dispersed over the ligand. In the  $D_3$  complex, additional phasing occurs for each ring vibration: three local A ring modes give rise to modes of  $A_1$  and E symmetry and three local B ring modes give rise to modes of  $A_2$  and E symmetry.

The VCD spectra observed for the tris(ethylenediamine) complexes cannot be interpreted in terms of coupled oscillator contributions,<sup>30-35</sup> which could arise from the chiral orientations of local  $NH_2$  or  $CH_2$  electric dipole transition moments in the allowed vibrational modes of the complex. The coupled oscillator mechanism predicts conservative bisignate VCD couplets for localized modes such as the symmetric or antisymmetric  $NH_2$  or  $CH_2$  stretches, which will be observed only if  $A_2, E$  pairs of exciton modes or A,B pairs of ring modes are split in frequency. Clearly, the observed VCD features in Figures 3-6 are monosignate, and the corresponding absorption bands show no evidence of exciton splitting.

The source of the monosignate, biased VCD observed for the various types of vibrational motion in  $[Co(en)_3]^{3+}$  must therefore be from an additional mechanism. If individual local motions generate an intrinsic magnetic dipole transition moment, the intrinsic VCD contribution from each localized mode will be observed in the VCD spectrum independent of any additional phasing among the set of local motions in the complex.<sup>28</sup> We thus only need to consider sources for intrinsic magnetic dipole transition moments.

Biased VCD features in the hydrogen stretching regions for a wide variety of molecules have recently been interpreted in terms of vibrationally generated ring currents.<sup>2-7</sup> According to this mechanism, the nuclear momentum of a driving oscillator can initiate current, which occurs at constant electron density, around a closed intramolecular loop. This current gives rise to a magnetic dipole transition moment which can be expressed as<sup>7</sup>

$$\left( \frac{\partial m^{\text{ring}}}{\partial P_a} \right)_{0,0} = \frac{1}{c} \left( \frac{\partial I^{\text{ring}}}{\partial P_a} \right)_0 \sum_{n \rightarrow l} \frac{1}{2} \mathbf{R}_n \times \mathbf{R}_l$$

where  $(\partial I^{\text{ring}} / \partial P_a)_0$  is the change in positive current in the ring due to the vibrational momentum and the summation is taken over consecutive  $n, l$  pairs of nuclei around the ring at positions  $\mathbf{R}_n$  and  $\mathbf{R}_l$ . Descriptively, the direction of  $(\partial m^{\text{ring}} / \partial P_a)_0$  can be found by using the right-hand rule for positive current flow around the ring.

The  $[Co(en)_3]^{3+}$  complex in solutions containing excess chloride ion contains rings which are closed either by metal coordination alone or by metal ligations and chloride bridging and which thus provide pathways for vibrational ring current. For all the vibrational modes of the complex having a complete enough descriptive assignment to establish the direction of the electric dipole transition moment  $\mu$ , the ring-current mechanism can be used to predict the sign of the VCD. Our interpretation considers intrinsic VCD due to current around the rings associated with a single ethylenediamine ligand or a single pair of chloride-bridged amino groups.

Enhancement of the NH stretching VCD in  $[Co(en)_3]^{3+}$  in  $Me_2SO-d_6$  containing excess chloride can arise from current

(30) Bosnich, B. *Acc. Chem. Res.* **1969**, *2*, 266.

(31) Holzwarth, G.; Chabay, I. *J. Chem. Phys.* **1972**, *57*, 1632.

(32) Keiderling, T. A.; Stephens, P. J. *J. Am. Chem. Soc.* **1977**, *99*, 8061.

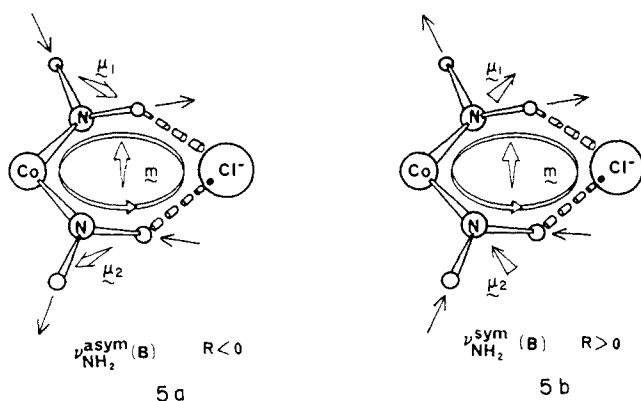
(33) (a) Su, C. N.; Keiderling, T. A. *J. Am. Chem. Soc.* **1980**, *102*, 511.

(b) Su, C. N. Ph.D. Thesis, University of Illinois-Chicago Circle, 1982.

(34) Heintz, V. J.; Keiderling, T. A. *J. Am. Chem. Soc.* **1981**, *103*, 2395.

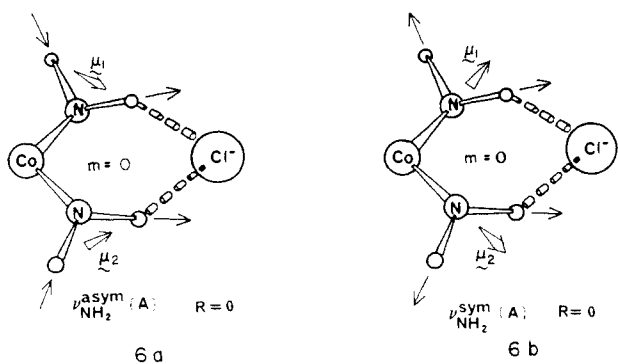
(35) Narayanan, U.; Keiderling, T. A. *J. Am. Chem. Soc.* **1983**, *105*, 6406.

generated around the chloride-bridged rings, as shown in **5a** and **5b**. For motions of the two NH<sub>2</sub> groups which are antisymmetric



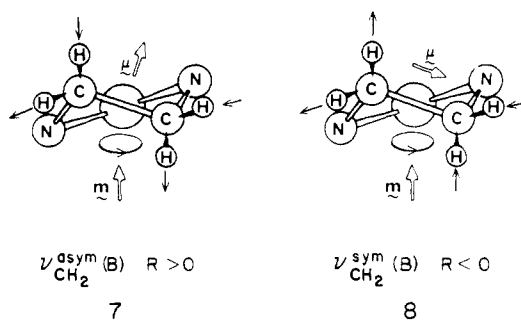
to rotation about the C<sub>2</sub> axis of the chloride-bridged ring (B symmetry), the concerted push-pull motion of the two Cl-bridged NH bonds drives electrons clockwise in the diagrams, initiating positive current around the closed ring in the counterclockwise direction shown by the loops in **5a** and **5b**. A magnetic dipole transition moment directed upward and out of the page is produced. Since NH elongation corresponds to an electric dipole transition moment with positive direction N → H,<sup>36</sup> the net electric dipole moment for the symmetric stretch also has a large upward component, and positive ring current enhanced rotational strength ( $R = \mu \cdot m$ ) is predicted for this mode. In the antisymmetric stretch, **5a**, the twist of the NH<sub>2</sub> groups, due to the  $\delta$  conformation of the ligand rings, results in a net electric dipole transition moment with a downward component, giving rise to negative ring current enhanced rotational strength.

For the two NH<sub>2</sub> stretches symmetric to C<sub>2</sub> rotation (A symmetry), **6a** and **6b**, the bridged NH hydrogens are moving in the same direction. No ring current can be generated around this ring by the motion of the bridged NH groups, and hence, zero

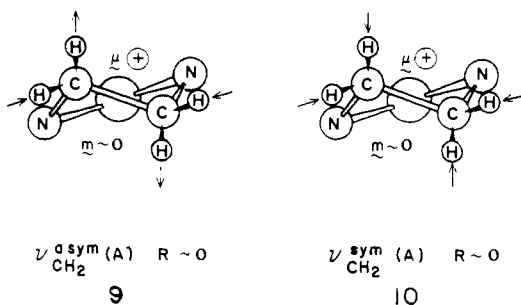


intrinsic rotational strength is predicted for the A modes. The ring-current mechanism therefore predicts negative VCD for the antisymmetric NH<sub>2</sub> stretches and positive VCD for the symmetric NH<sub>2</sub> stretches, due to current generated in the Cl-bridged rings, in agreement with experiment (Figure 3). The positive VCD at 3180 cm<sup>-1</sup> is likely due to Fermi resonance borrowing of VCD intensity from the symmetric stretch by an overtone or combination band involving the NH<sub>2</sub> scissors mode, as also suggested for the NH stretching region in Co(acac)<sub>2</sub>(L-ala).<sup>6</sup>

The ring-current interpretations for the methylene stretching modes of [Co(en)<sub>3</sub>]<sup>3+</sup> are shown in **7-10**. The relevant ring for these modes is the ligand ring, since the CH bonds are not interacting strongly with the chloride. For CH elongation, positive  $\mu$  is directed H → C.<sup>36</sup> In the antisymmetric and symmetric stretches of B symmetry, **7** and **8**, respectively, the pair of equatorial hydrogen nuclei are moving in a concerted fashion, such that one CH bond is elongating while the other is contracting,



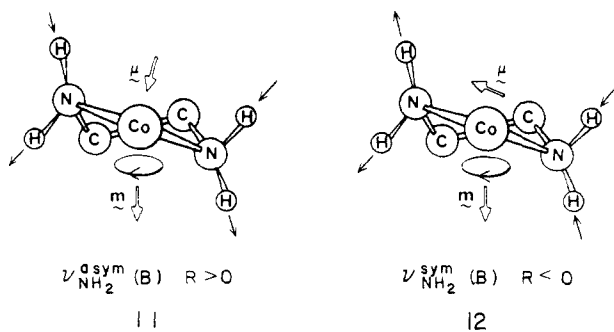
which results in electron flow along the C-C bond joining the two methylenes. Each equatorial CH bond is trans to and approximately coplanar with covalent bonds in the ring, and the nuclear momenta of the equatorial hydrogens are in the approximate ring plane. Thus motion of the equatorial CH groups influences the motion of the electrons in the C-N and Co-N bonds. The predominant electron flow generated along the C-C bond by the equatorial CH stretches dictates the sense of flow of current (at constant electron density) which is initiated around the ring. The axial hydrogens are also moving in a concerted fashion which causes electron flow along the C-C bond. However, since the momenta of the axial hydrogens are transverse to the ring plane, this C-C bond flow should lead only to charge redistribution in the axial CH groups rather than ring current. Thus in the antisymmetric stretch **7**, positive ring current due to the equatorial CH motion results in a magnetic dipole transition moment directed upward, and since  $\mu$  also has an upward component, positive VCD is predicted. Reversing the phase of the axial CH motions gives rise to the symmetric stretch **8**, for which  $\mu$  has a downward component, and negative VCD is predicted. In the A symmetry modes, **9** and **10**, the motions of the pair of axial or equatorial



CH groups oppose one another, and no net charge flow along the C-C bond can result. No ring-current VCD contribution arises from the ligand A methylene stretches. The ring-current mechanism thus predicts positive VCD in the antisymmetric CH<sub>2</sub> stretching region and negative VCD in the symmetric stretching region for the  $\delta$  conformation, in agreement with the observed spectra of  $\Lambda$ -[Co(en)<sub>3</sub>]<sup>3+</sup> and  $\Lambda$ -[Cr(en)<sub>3</sub>]<sup>3+</sup> in Me<sub>2</sub>SO-d<sub>6</sub>, D<sub>2</sub>O, and acidic D<sub>2</sub>O solutions.

Similar interpretation of the VCD intensity based on current in the chelate ring can be made for other spectral regions in  $\Lambda$ -[Cr(en)<sub>3</sub>]<sup>3+</sup> and  $\Lambda$ -[Co(en)<sub>3</sub>]<sup>3+</sup>. In the NH stretching region for D<sub>2</sub>SO<sub>4</sub>/D<sub>2</sub>O solutions, the antisymmetric NH<sub>2</sub> stretches give rise to positive VCD intensity and the symmetric NH<sub>2</sub> stretches to negative VCD intensity, the same signs as the corresponding CH<sub>2</sub> stretching modes. In this solution, the CH stretching VCD is indicative of an excess of the  $\delta$  ring conformation, but the anion bridges between NH<sub>2</sub> groups apparently are not present. As shown for the B modes in **11** and **12**, VCD with the observed sign can arise from a magnetic dipole transition moment due to ring current in the chelate ring. The concerted push-pull motion of the two equatorial NH bonds must direct electrons through the N-C-C-N portion of the ring to generate the desired sense of positive ring current in both B modes. The directions of the momenta of the two equatorial NH bonds do in fact correspond to counterclockwise circulation in **11** and **12**, which can account for the current sense.

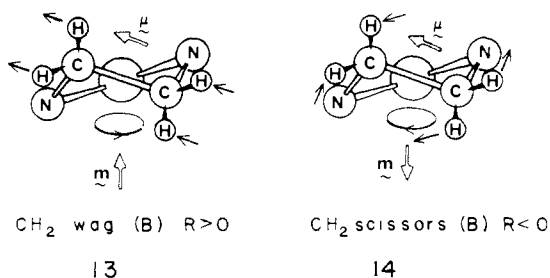
(36) Wiberg, K. B.; Wendoloski, J. J. *J. Phys. Chem.* **1984**, *88*, 586.



The modes of A symmetry cannot produce ring-current magnetic moments.

We have proposed two separate ring-current-mechanism pathways for the  $\text{NH}_2$  stretching modes which give rise to VCD of opposite sign. From the spectra in the two extreme cases,  $\text{D}_2\text{SO}_4$  solution and  $\text{Me}_2\text{SO}-d_6$  with excess chloride, we find that the observed ring-current enhancement for the symmetric  $\text{NH}_2$  stretching VCD is smaller than that for the antisymmetric  $\text{NH}_2$  stretch for the ligand ring pathway but larger than that for the antisymmetric  $\text{NH}_2$  stretch for the chloride bridge pathway, due to the orientations of the  $\text{NH}_2$  groups with respect to the two types of ring. Furthermore, larger ring-current magnetic moments are produced by the chloride-bridged ring than by the ligand ring. Therefore, as the number of chloride-bridged  $\text{NH}_2$  groups increases (e.g., as  $\text{Cl}^-$  is added to a solution of the iodide salt), the symmetric stretching VCD changes sign first. The superposition of the two types of  $\text{NH}$  stretching ring-current contribution is apparent in Figures 1 and 5. In  $\text{Me}_2\text{SO}-d_6$ , the weak positive VCD in both the symmetric and antisymmetric  $\text{NH}_2$  stretching regions for the iodide salt is suggestive of some slight bridge formation by iodide.

The monosignate VCD features observed in the mid-infrared region of  $[\text{Co}(\text{en})_3]^{3+}$  in  $\text{Me}_2\text{SO}-d_6$  with excess chloride provide the opportunity to extend the application of the ring-current mechanism to bending motions. The modes at 1460 and 1377  $\text{cm}^{-1}$  are localized modes which have major contributions from methylene scissors and wagging motions, respectively, and therefore the direction of the electric dipole transition moment can be determined. The  $\text{CH}_2$  scissors and wag having B symmetry for a single ligand are shown in 13 and 14. In both cases, the



direction of positive  $\mu$  is determined by the direction of the hydrogen motion<sup>36</sup> and results in a moment pointing to the left along the C-C bond direction. Due to the pucker of the ring, in both the wag and scissors, the motions of the equatorial hydrogens have components in the projected ring plane. For these bending modes, it is proposed that the concerted motion of the equatorial CH bonds determines the direction of electron flow; that is, when the equatorial CH hydrogens have net motion to the right, electron flow is initiated along the C-C bond and around the ring to the right and vice versa. The positive ring currents and resulting magnetic dipole transition moments shown in 13 and 14 gave rise to negative ring-current VCD in the  $\text{CH}_2$  scissors mode and positive ring-current VCD in the  $\text{CH}_2$  waggings mode, as observed. In the wag, the axial CH hydrogen motion initiates ring current which reinforces the equatorial hydrogen ring current, whereas in the scissors mode, the action of the axial CH hydrogens opposes the presumably larger effect of the equatorial CH hydrogens which are in the plane of the ring bonds. In axial CH contribution

may thus diminish the enhancement of the scissors mode. The weaker positive feature at 1397  $\text{cm}^{-1}$  probably arises from Fermi resonance intensity borrowing from the 1377- $\text{cm}^{-1}$  wag.

The remaining three distinct VCD features (Figure 4) observed at 1332 (-), 1285 (+), and 1215  $\text{cm}^{-1}$  (-) are less definitively assigned. The higher frequency modes in this group probably arise from a mixture of methylene and amino twist and rock. The strong monosignate nature of the VCD is indicative of ring current, which can again be initiated by the concerted motion of equatorial CH and NH groups. The mode at 1215  $\text{cm}^{-1}$  has a weak absorption intensity and large VCD, resulting in an anisotropy ratio of -0.01, one of the largest observed to date. This band cannot be primarily  $\text{NH}_2$  twist or rock, since it apparently does not shift significantly upon deuteration in similar complexes.<sup>27</sup> As discussed above, a contribution from nitrogen motion is likely. A possible assignment is the antisymmetric ring CN stretching mode (B symmetry). Since the two CN bonds are fairly coplanar, the dipole strength should be small, whereas antisymmetric motion within the ring itself (similar to the motion of the chloride-bridged NH groups in 5a and 5b) may generate quite large ring currents. Weak absorptions with a large anisotropy ratio have also been observed in this region in six-membered-ring compounds.<sup>37</sup>

### Conclusions

The studies presented here on tris-chelated complexes of Co(III) and Cr(III) with ligands having only conformational chirality have demonstrated the usefulness of vibrational circular dichroism as a direct probe of chelate ring conformation. For quantitative application, the VCD spectrum of a known conformation or conformational mixture must be available. In addition, vibrational modes must be present whose VCD intensity arises only from the conformational chirality and is not affected by external conditions which cause variation in the ring conformations. For the ethylenediamine ligand, the methylene stretching VCD bands satisfy these criteria in  $\text{D}_2\text{O}$  solution. For  $[\text{Co}(\text{en})_3]^{3+}$  and  $[\text{Cr}(\text{en})_3]^{3+}$ , the presence of chloride or bromide counterion was found to influence the solution ring conformation due to formation of hydrogen-bonded bridges in both aqueous and  $\text{Me}_2\text{SO}$  solutions. This degree of conformation detail for solution samples is not readily attainable from techniques other than VCD. The specific type of internal association with three halide ions described here for these complexes has not been previously proposed, particularly for aqueous solutions, although proton NMR and difference CD spectra of *cis*- $\text{Co}(\text{en})_2\text{X}_2$  salts in  $\text{Me}_2\text{SO}$  have been interpreted in terms of a single anion bridge between adjacent ethylenediamine ligands.<sup>38</sup>

The utility of VCD in deriving the conformational structures discussed here is due to the occurrence of large, monosignate VCD features which can be associated with specific types of vibrational motions able to generate ring currents. The sign of ring-current-enhanced VCD for a given molecular conformation can be predicted on the basis of empirical rules which can be consistently applied to a wide variety of molecular structures.<sup>2-6</sup> From our previous investigations, we have devised rules for ring current generated by hydrogen stretching motion for a single XH oscillator ( $X = \text{C}, \text{N}, \text{O}$ ) within a hydrogen-bonded ring and for a single CH oscillator adjacent to a heteroatom in a closed ring.<sup>2,5</sup> Our analysis of the ring-current-enhanced VCD in the ethylenediamine chelate ring and chloride-bridged ring has provided a third example of nuclear momenta which can generate ring current, the concerted out-of-phase motion of a pair of CH or NH bonds which are equatorial to the ring. In the CH stretching region, the elongation of one bond and contraction of the other results in electron flow along the C-C bond, which initiates ring current. In the CH bending region, electron flow around the ring corresponds to the sense of motion of the equatorial hydrogens in the ring plane. Ring-current generation by the concerted out-of-phase motions of the two ethylenediamine  $\text{NH}_2$  groups has also been proposed

(37) Lipp, E. D.; Nafie, L. A. *Appl. Spectrosc.* **1984**, *38*, 20.

(38) (a) Nakazawa, H.; Sakaguchi, U.; Yoneda, H.; Morimoto, Y. *Inorg. Chem.* **1981**, *20*, 973. (b) Nakazawa, H.; Sakaguchi, U.; Yoneda, H. *J. Am. Chem. Soc.* **1982**, *104*, 3885.



to explain the VCD. For amino vibrations, current can be generated both in the ligand ring and in the ring closed by a bridging halide ion. The VCD spectra of these metal complexes appear to be completely dominated by ring-current effects, which mask any coupled oscillator VCD contributions.

Further examples of ring-current-enhanced VCD in transition-metal complexes have been observed for  $\beta$ -alanine ligands, which form six-membered rings,<sup>39</sup> and  $\alpha$ -amino acid ligands, which form five-membered chelate rings.<sup>40</sup> These results, which will

be reported separately, confirm and extend the mechanisms proposed here for the CH and NH stretching VCD of ethylenediamine ligands.

**Acknowledgment.** We acknowledge financial support from grants from the National Science Foundation (CHE83-02416) and the National Institutes of Health (GM-23567). We are grateful to Faye Ratnowsky for carrying out some of the syntheses and resolutions of the cobalt complexes.

(39) Freedman, T. B.; Young, D. A.; Nafie, L. A., unpublished results.

(40) Freedman, T. B.; Young, D. A.; Oboodi, M. R.; Nafie, L. A., submitted for publication.

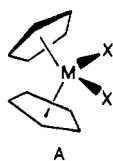
## Aqueous Coordination Chemistry of Vanadocene Dichloride, $V(\eta^5-C_5H_5)_2Cl_2$ , with Nucleotides and Phosphoesters. Mechanistic Implications for a New Class of Antitumor Agents

Jeffrey H. Toney,<sup>†</sup> Carolyn P. Brock, and Tobin J. Marks\*

Contribution from the Department of Chemistry, Northwestern University, Evanston, Illinois 60201. Received March 14, 1986

**Abstract:** This paper reports an investigation of the mode of interaction of the organometallic antitumor agent  $Cp_2VCl_2$  ( $Cp = \eta^5-C_5H_5$ ) with nucleotides and phosphoesters, in aqueous solution near physiological pH, employing high-field  $^1H$  and  $^{31}P$  FT NMR and EPR. Paramagnetic ( $d^1$ ) aqueous  $Cp_2VCl_2$  is found to selectively interact with the phosphate functionalities of nucleotides and to significantly shorten the  $^{31}P$  nuclear relaxation times. A quantitative analysis of the paramagnetic contributions to the longitudinal ( $T_1$ ) and transverse ( $T_2$ ) relaxation rates of the  $^{31}P$  nucleus of 2'-deoxyadenosine-5'-monophosphate reveals that the average internuclear vanadium-phosphorus distance in the solution complex is 6.2 (2) or 5.5 (1) Å, depending on whether each vanadium ion interacts with one or two phosphate moieties, respectively. The temperature dependence of the  $^{31}P$  relaxation rates yields kinetic parameters characterizing the labile outer-sphere complexation of aqueous  $Cp_2VCl_2$  to the phosphate groups. At 25 °C, the mean lifetime of the metal-nucleotide complex is estimated to be 0.49 (8) ms. Activation parameters for the ligand dissociation at 25 °C are the following:  $\Delta G^\ddagger = 19.5$  (2.6) kcal/mol,  $\Delta H^\ddagger = 13.8$  (1.0) kcal/mol, and  $\Delta S^\ddagger = -19.1$  (4.3) e.u. Nucleotide-nucleotide Watson-Crick base-pairing is not disrupted by  $Cp_2VCl_2$  in aqueous solution, as shown by  $^1H$  NMR. An X-ray crystallographic study was also carried out on the model compound,  $Cp_2V(OH_2)_2 \cdot 2O_2P(OPh)_2$  (**1**). The crystal structure of **1** serves to define the coordination of the  $Cp_2V^{2+}$  unit to a diesterified phosphoric acid, which possesses metrical parameters similar to those of polynucleotides. The complex crystallizes in the monoclinic space group  $P2_1$  (No. 4) with four molecules in a unit cell of dimensions  $a = 10.571$  (2) Å,  $b = 12.108$  (3) Å,  $c = 25.277$  (6) Å, and  $\beta = 98.50$  (2)° at 163 (2) K. Least-squares refinement led to a value for the conventional  $R$  index (on  $F$ ) of 0.031 for 6197 unique reflections having  $2\theta_{MoK\alpha} \leq 55^\circ$  and  $I > 3\sigma(I)$ . The molecular structure consists of pseudotetrahedral  $V(\eta^5-C_5H_5)_2(OH_2)_2^{2+}$  cations connected to diphenyl phosphate anions via strong hydrogen bonds. Average metrical parameters for the  $V(\eta^5-C_5H_5)_2(OH_2)_2^{2+}$  cation are as follows: V-C distance, 2.297 (5) Å; V-O(water) distance, 2.050 (8) Å; ring centroid-V-ring centroid angle, 133.0 (4)°. Average metrical parameters for the  $PO_2(OPh)_2^-$  anion are P-OPh distance, 1.601 (6) Å; P-O (non-ester), 1.480 (2) Å; and C-O distance, 1.392 (3) Å, and these are typical for a phosphodiester anion. The vanadium-phosphorus nonbonded contacts are in the range 5.07-6.44 Å, in good agreement with the nucleotide NMR results in solution. Implications of these results for the observed biological activity of  $Cp_2VCl_2$  are briefly discussed.

Köpf and Köpf-Maier have shown that metallocene dihalides and bis(pseudohalides) of the constitution  $Cp_2MX_2$  (A) where  $Cp = \eta^5-C_5H_5$ ,  $M = Ti, V, Nb, Mo^{1-6}$ ;  $X = F, Cl, Br, I, NCS$ , and  $N_3$ ,<sup>7</sup> are highly active agents against Ehrlich ascites tumor (EAT) cells, lymphoid leukemia L1210, lymphocytic leukemia P388,<sup>8</sup> and most recently, human colon carcinoma heterotransplanted to athymic mice.<sup>9</sup> In addition, we have recently shown



that  $Cp_2VCl_2$  is highly active against human epidermoid (HEP-2) tumor cells in vitro as well as intraperitoneal (ip) implants of a

- (1) Köpf, H.; Köpf-Maier, P. *Angew. Chem., Int. Ed. Engl.* **1979**, *18*, 477-478.
- (2) Köpf-Maier, P.; Hesse, B.; Köpf, H. *J. Cancer Res. Clin. Oncol.* **1980**, *96*, 43-51.
- (3) Köpf-Maier, P.; Köpf, H. *Z. Naturforsch. B.: Anorg. Chem., Org. Chem.* **1979**, *34b*, 805-807.
- (4) Köpf-Maier, P.; Leitner, M.; Köpf, H. *J. Inorg. Nucl. Chem.* **1980**, *42*, 1789-1791.
- (5) Köpf-Maier, P.; Leitner, M.; Voigtländer, R.; Köpf, H. *Z. Naturforsch. B.: Anorg. Chem., Org. Chem.* **1979**, *34c*, 1174-1176.
- (6) Köpf-Maier, P.; Hesse, B.; Voigtländer, R.; Köpf, H. *J. Cancer Res. Clin. Oncol.* **1980**, *97*, 31-39.
- (7) Köpf-Maier, P.; Wagner, W.; Hesse, B.; Köpf, H. *Eur. J. Cancer* **1981**, *17* (6), 665-669.
- (8) Köpf-Maier, P.; Wagner, W.; Köpf, H. *Cancer Chemother. Pharmacol.* **1981**, *5*, 237-241.

<sup>†</sup> Present address: Laboratory of Biochemical Pharmacology, Dana-Farber Cancer Institute, Harvard Medical School, Boston, MA 02115.